Non-viral *Smad7* gene delivery and attenuation of postoperative peritoneal adhesion in an experimental model

H. Guo[1], J. C. K. Leung[1], J. S. Cheung[2,3], L. Y. Y. Chan[1], E. X. Wu[2,3] and K. N. Lai[1]

[1]Department of Medicine, Queen Mary Hospital, [2]Laboratory of Biomedical Imaging and Signal Processing, [3]Department of Electrical and Electronic Engineering, University of Hong Kong, Hong Kong

Correspondence to: Professor K. N. Lai, Department of Medicine, University of Hong Kong, Room 409, Professorial Block, Queen Mary Hospital, 102 Pokfulam Road, Hong Kong (e-mail: knlai@hkucc.hku.hk)

Tel: [852]-28554251

Fax: [852]-28162863

Short Running Title: *Smad7* inhibits postoperative peritoneal adhesion

ABSTRACT

Background: Postoperative intra-abdominal adhesion is associated with high morbidity and mortality. Smad7, a protein that occupies a strategic position in fibrogenesis, inhibits the transforming growth factor (TGF) β/Smad signalling pathway. In this study the therapeutic potential of exogenous Smad7 in preventing fibrogenesis in postoperative intra-abdominal adhesion was investigated.

Methods: Intra-abdominal adhesion was induced in a rodent model by peritoneal abrasion. ***Smad7*** **[Author's response: We have checked that Smad7 has been correctly italicized when relating to the *Smad7* gene.]** was delivered into the peritoneal cavity by a non-viral ultrasound–microbubble-mediated naked gene transfection system. **The effect of *Smad7* transgene on adhesion formation was studied by measuring the changes of TGF-β, fibrogenic factors, α-SMA, and Smad2/3 activation in the anterior abdominal wall.**

Results: Four weeks after surgical abrasion, all rats developed significant peritoneal adhesion with enhanced TGF-β expression, increased levels of extracellular matrix components and activated myofibroblasts, accompanied by decreased *Smad7* expression and increased Smad2/3 activation. In rats treated with the *Smad7* transgene, the incidence and severity of peritoneal adhesion were significantly reduced with biochemical downregulation of fibrogenic factors and inhibition of Smad2/3 activation. Serial

quantitation using magnetic resonance imaging revealed a significant reduction in adhesion areas ~~by **50–70 per cent**~~ from day 14 onwards.

Conclusion: Ultrasound–microbubble-mediated gene transfection is an effective, safe and controllable technique that provides timely targeted gene delivery for the treatment of postoperative peritoneal adhesions.

Introduction

The development of adhesions is generally considered inevitable after abdominal surgery. More than 95 per cent of abdominal operations result in intra-abdominal adhesions, although the frequency with which these cause problems is not clear[1]. Postoperative intra-abdominal adhesions are associated with bowel obstruction, inadvertent enterotomy at adhesiolysis, secondary female infertility, extended operating time and increased intraoperative complications in subsequent surgery, and, most importantly, increased mortality[2]. Furthermore, postoperative intra-abdominal adhesions have a huge impact on health costs[3] and medicolegal litigation[4]. Various anti-adhesion strategies, including laparoscopic surgery, chemical and mechanical separation of bowel loops, and inhibition of fibrin deposition or fibroblast proliferation, have been employed to prevent postoperative peritoneal adhesion, with limited success[5,6]. Clinical studies of the efficacy of adhesion-limiting agents have been difficult to evaluate because of the inherent problem of determining the presence, reduction or absence of adhesions serially within the intact abdomen of patients or experimental animals.

Postoperative adhesions represent exaggerated and dysregulated peritoneal 'repair' mechanisms in response to trauma, leading to a series of local responses involving acute inflammation, extracellular matrix (ECM) deposition, fibrinolysis and neoangiogenesis[7,8]. It is increasingly recognized that the transforming growth factor (TGF) β/Smad signalling

pathway plays an important role in the development of fibrosis[9]. Other than abdominal surgery, similar peritoneal adhesions occur following abdominopelvic radiation therapy[10]. Overexpression of *Smad7* attenuates the fibrotic effect of TGF-β in renal tubular epithelial cells and prevents tissue fibrosis in the kidney[11,12]. Recently, the authors successfully delivered the *Smad7* transgene into the peritoneal tissues by a non-viral ultrasound–microbubble-mediated system[13]. In the present study, intraperitoneal gene transfer of *Smad7* to block the TGF-β/Smad signalling pathway was employed in a surgical peritoneal adhesion model, with histological and pathophysiological evaluation of this approach, as a potential method of reducing postoperative abdominal adhesion.

Methods

Animal model of peritoneal adhesion

All animal studies were conducted with the approval and guideline of Committee on the Use of Live Animals in Teaching and Research of the University of Hong Kong. All experiments conformed to the University's animal care protocols and all surgical procedures were conducted under aseptic conditions in the Laboratory Animal Unit.

A surgically induced abdominal adhesion model was developed in healthy male Sprague Dawley rats weighing 200–250 g, using a technique modified from that of Chung *et al*[14]. In brief, a 3-cm vertical midline incision was made through the abdominal wall and peritoneum. Both dorsal and ventral surfaces of the caecum were exposed and abraded with a size 15 scalpel blade until blood appeared on the caecal surface. The caecum was then placed back into the abdominal cavity in its natural position. The parietal peritoneum lateral to the midline incision was also scraped 30 times until petechial haemorrhages were observed. Subsequently, the abdominal incision was closed in two layers with 4/0 silk sutures. Sham-operated controls were subjected to midline incision of the abdomen without any scraping.

Preparation of naked plasmid DNA

Mouse *Smad7* cDNA with a flag tag (m2) at its amino terminus in pcDNA3 (a gift from Dr H. Zhu, Ludwig Institute for Cancer Research, Victoria, Australia) was subcloned into

a tetracycline-inducible vector, pTRE (Clontech, Palo Alto, California, USA), to obtain pTRE–m2*Smad7*. To achieve doxycycline-induced *Smad7* transgene expression, pTRE–m2*Smad7* and an improved pTet-on vector (Clontech), pEFpurop-Tet-on (a gift from Dr G. Vario, Cerylid, Melbourne, Australia), were co-transfected into the peritoneal cavity using ultrasound-guided delivery. The plasmid DNA obtained from *Escherichia coli* DH5α culture was purified with the Qiagen Plasmid Maxi kit (Qiagen, Valencia, California, USA). The identity and purity of the plasmid DNA were confirmed by 1 per cent agarose gel electrophoresis before and after digestion with restriction endonucleases.

Gene transfer of inducible* Smad7 *into the peritoneal cavity

Exogenous *Smad7* was delivered into the peritoneal cavity via an ultrasound–microbubble-mediated system[13]. Plasmid DNA including an equal amount of pTRE–m2*Smad7* and pEFpurop-Tet-on was dissolved in 0.9 per cent saline. Phospholipid-stabilized microbubbles (SonoVue®; Bracco Diagnostics, Princeton, New Jersey, USA) were gently resuspended before each aliquot was withdrawn. Prepared plasmids and the SonoVue® were mixed in ratio of 1 : 1 (vol : vol). Based on the authors' previous studies[13], the effect of *Smad7* gene transfer is dose dependent, with an optimal dose of 100 μg per rat. The degree of peritoneal *Smad7* expression is also time dependent, with a peak on days 2–7, reducing to baseline level on day 14 after ultrasound-mediated gene transfer.

In this study, 4 ml of the mixed solution containing 100 μg plasmids was injected immediately into the abdominal cavity. The ultrasound transducer (Sonitron ® **[Author: Please advise whether this, or any other product, has ® or ™.][Author's response: Sonitron 1000, which is similar to Sonitron 2000 from the same company, has a mark of ®]** 2000; Rich-Mar, Inola, Oklahoma, USA) was applied directly on to the abdominal wall with an input frequency of 1 MHz, a 20 per cent duty cycle and an output intensity of 2 W/cm^2 for a total of 30 s, with 75-s intervals in two cycles. The ultrasound probe was moved over the abdominal surface, from the costal margin to the pubic symphysis, to ensure that the ultrasound beam reached the whole peritoneum for effective delivery of the *Smad7* gene to the animal. After the application of ultrasound, *Smad7* transgene expression was induced by 1 ml doxycycline (500 μg/ml; Sigma, St Louis, Missouri, USA) via intraperitoneal injection, and continued by administering doxycycline 200 μg/ml in daily drinking water until the end of the experiment.

Experimental design

Animals were randomly divided and treated as follows: group 1, normal sham-operated controls (n=8); group 2, surgical abrasion but no other treatment (n=8); group 3, surgical abrasion plus ultrasound (n=6); group 4, surgical abrasion plus *Smad7* (n=7); group 5, surgical abrasion plus ultrasound and *Smad7* (n=10); group 6, surgical abrasion plus ultrasound and empty vectors with no *Smad7* (n=9). In group 5, the treatment was

performed on days 1 and 14 after surgery to ensure effective transfection, as a previous study had shown that peak gene expression of exogenous *Smad7* in peritoneal tissues occurred on the second day of transfection and that transgene expression decreased in a time-dependent manner[13]. Rats in groups 3, 4 and 6, serving as treatment controls, received the treatment at the same timepoint as animals in group 5, as appropriate. Four weeks after operation, animals were killed by anaesthesia for evaluation of adhesions and tissue collection.

Serial determination of peritoneal adhesions was **separately** studied by **a novel magnetic resonance imaging (MRI) technique developed recently in the authors' laboratory**[15], on days 7, 14, 21 and 28 after operation in three additional groups:**[Editor's question: Do you mean by "three additional groups" that these animals were in addition to the numbers given in the paragraph above?] [Author's response: Yes, these animals were additional to the numbers given in the paragraph above]** normal sham-operated controls (*n*=4); adhesion but no treatment (*n*=6); and adhesion treated with ultrasound–microbubble-mediated *Smad7* transfection as described above (*n*=6). **[Editor's question: Please clarify whether you are referring to groups 1, 2 & 5, respectively, as described above.] [Author's response: These animals were additional to the numbers of group 1, 2, & 5. The results of these animals are presented in Figure 2e illustrating the serial measurement of adhesion area by MRI.**

The method of inducing adhesion and giving Smad7 treatment were "as described above"]

Evaluation of adhesion formation and tissue collection

Surface areas of peritoneal adhesion were measured serially by abdominal MRI as described previously[15]. In brief, each animal received an intraperitoneal injection of prewarmed peritoneal dialysate (0.1 ml/g; Fresenius Medical Care, Bad Homburg, Germany) as contrast medium after overnight fasting to reduce intestinal motion during MRI. MRI was performed using a small-animal MRI scanner with maximum gradient of 360 mT/m (70/16 PharmaScan; Bruker BioSpin GmbH, **Ettlingen,** Germany), operating at 7 T. Axial and sagittal gradient echo images were acquired by a multislice flow-compensated two-dimensional gradient echo sequence with the following parameters: repetition time 1 s, echo time 3.5 ms, acquisition matrix 192 × 192, flip angle 30°, field of view 6.0 × 6.0 cm, slice thickness 1.0 mm, slice gap 0.5 mm, number of slices 16–22, number of **averaging** 2. The mean duration for each image was 15 min. The boundary of the peritoneal adhesion near the caecum was segmented for each animal in the multislice image data set obtained after MRI. The corresponding adhesion area was calculated from the estimated length of the adhesion boundary on each slice and the centre-to-centre slice spacing by two blinded observers. MRI measurements of adhesion surface areas correlate well with laparotomy estimates ($R = 0.99$)[15].

After death, the abdomen was opened through a U-shaped incision to prevent any disruption of adhesions. Adhesion formation was scored macroscopically on a scale of 0–4 according to their quantity and intensity by two independent observers. The Yilmaz classification was used to grade the adhesion[16]: grade 0, no adhesion; grade 1, thin adhesive bands, easily removable; grade 2, thick adhesive bands limited to one area; grade 3: extensive and thick adhesive bands; grade 4: extensive and thick adhesive bands, and adhesions between viscera and/or abdominal wall with difficult lysis. Adhesion surface area was estimated by measuring the representative lengths according to the shape of the adhesion, by two independent observers.

After evaluation of adhesions, an equal area of tissue was collected from the anterior abdominal wall at an identical position in all rats. Part of each tissue was fixed in 10 per cent neutral buffered formalin or frozen in optimal cutting temperature medium (Tissue-Tek®; Sakura Finetek, Torrance, California, USA) for histological and immunohistochemical evaluation. The remainder was kept at −70°C for total RNA and protein extraction.

Histology

After deparaffinization and rehydration, all sections (5-μm thick) of the anterior abdominal wall were stained with a modified Gomori's trichrome stain kit (Biocare Medical, Walnut Creek, California, USA). The peritoneal sections were examined in a

blinded manner and the thickness (in micrometers) of the submesothelial layer at five random locations was measured. Haematoxylin and eosin staining was also performed to evaluate inflammation in the anterior abdominal wall.

Immunofluorescence and immunohistochemistry staining

Immunohistochemical analysis and immunofluorescence staining (for determination of flag m2 protein, TGF-β, α-smooth muscle actin, collagen I, collagen III and fibronectin) in the abdominal wall were performed using paraffin-embedded or frozen sections as appropriate[17]. The bound antibodies were detected by means of Dako Envision Plus kits (Dako, Carpinteria, California, USA) or FITC-conjugated antimouse antibodies as appropriate.

RNA isolation and reverse transcriptase–polymerase chain reaction

RNA extraction and RT–PCR were performed as described previously[17]. The primer sequences for amplifying the target genes, the Genebank accession number and their product sizes are as follows: rat collagen I (Z78279, 469 bp), 5′-TGCCGTGACCTCAAGATGTG-3′ (forward) and 5′-CACAAGCGTGCTGTAGGTGA-3′ (reverse); rat collagen III (NM_032085, 482 bp), 5′-CTGGACCAAAAGGTGATGCTG-3′ (forward) and 5′-TGCCAGGGAATCCTCGATGTC-3′ (reverse); rat fibronectin (NM_019143, 320 bp), 5′-GAAGTGGTTCATGCCGATCA-3′ (forward) and 5′-TCCAGCCCTGTAACTGTGTA-3′

(reverse); rat α-smooth muscle action (α-SMA) (J02781, 101 bp), 5′-AAGAGGAAGACAGCACAGCTC-3′ (forward) and 5′-GAT GGATGGGAAAACAGCC-3′ (reverse); rat Smad2 (AF056001, 477 bp), 5′-CACAAGCGTGCTGTAGGTGA-3′ (forward) and 5′-CACTATCACTTAGGCACTCG-3′ (reverse); rat TGF-β1 (NM_021578, 301 bp), 5′-GCAACAACGCAATCTATGAC-3′ (forward) and 5′-CCCTGTATTCCGTCTCCTT-3′ (reverse); and glyceraldehyde-3-phosphate dehydrogenase (GAPDH) (AB017801, 837 bp), 5′-ACCCCTTCATTGACCTCAACT-3′ (forward) and 5′-ACCAGGAAATGAGCTTCACAAA -3′ (reverse). GAPDH served as an internal control. The PCR product yielded was expressed as a ratio to the GAPDH amplicon.

Real-time polymerase chain reaction for* Smad7 *mRNA quantification

After total RNA extraction, cDNA was synthesized from DNase-treated total RNA (2 μg) in 20-μl reactions using the Superscript II reverse transcriptase kit (Invitrogen, Carlsbad, California, USA) and stored at −20°C until use. *Smad7* qPCR primers used were: 5′-CCAACTGCAGACTGTCCAGA-3′ (forward) and 5′-TTCTCCTCCCAGTATGCCAC-3′ (reverse); GAPDH qPCR primers were: 5′-TGCCACTCAGAAGACTGTGG-3′ (forward) and 5′-GGATGCAGGGATGATGTTCT-3′ (reverse). Real-time PCR reactions were carried out in an ABI Prism 7500 Sequence Detection system using the SYBR-Green reaction kit (Applied Biosystems, Foster City, California, USA). For quantification,

GAPDH mRNA served as an endogenous control. The ΔΔCt method was used to calculate the results.

Western blot analysis

Tissue from the anterior abdominal wall was ground and homogenized in a lysis buffer before subjecting to western blot analysis with specific antibodies, as described previously[17]. The primary antibodies included mouse monoclonal antibodies to actin (1 : 2000; Lab Vision Corporation, Fremont, California, USA), α-SMA (1 : 2000; Dako) and fibronectin (1 : 1000; Fitzgerald Industries, Concord, Massachusetts, USA), goat polyclonal antibodies to pSmad2/3 (1 : 600), rabbit polyclonal antibodies to Smad2 and TGF-β1 (1 : 600; Santa Cruz Biotechnology, Santa Cruz, California, USA), collagen I (1 : 20 000) and collagen III (1 : 10 000; Fitzgerald Industries). The secondary antibodies included a 1 : 20 000 dilution of horseradish peroxidase-conjugated swine antigoat (for pSmad2/3), a 1 : 30 000 dilution of goat antimouse (for actin, α-SMA and fibronectin) and a 1 : 2000 dilution of goat antirabbit (for collagen I, collagen II, TGF-β1 and Smad2) antibodies (Dako). Densitometry results were reported as a ratio to the actin signal.

Statistical analysis

Data for *Smad7* expression in the peritoneum were expressed as mean (s.d.) and analysed by Tukey's multiple comparison test. The results of fibrogenic factors and the thickness of the submesothelial layer of peritoneum were expressed as median (interquartile range)

and analysed by non-parametric methods. Differences in these parameters between the study groups were compared with the Kruskal–Wallis test, and differences between individual groups with the Mann–Whitney *U* test. **Differences in MRI-measured adhesion area between adhesions with no treatment and *Smad7*-treated groups were compared with t-test.** Correlations between MRI-measured adhesion area and laparotomy estimation, as well as bodyweight, were evaluated with Pearson's correlation test. $P < 0.050$ was considered statistically significant. Analyses were performed with the statistical package SPSS® version 12.0 (SPSS, Chicago, Illinois, USA).

Results (Editor's remark: I am conscious that there are a lot of Figures in your manuscript. Where possible, text and illustration should be complementary rather than merely duplicative. For this reason, I suggest that we omit the histology pictures (Figs 3 a-c) and the immunohistochemistry (Figs 5 a-c) and simply retain the text. Please confirm that you would be happy with these changes. Adjust the numbering of subsequent figures accordingly.) [Author's response: Figs 3 and Figs 5 were omitted as you suggested. We would be happy with these changes. The numbering of subsequent figures has been adjusted (in bold).]

Smad7 ***transfection rate and transgene expression in the peritoneum***

After the delivery of *Smad7* transgene, expression of *Smad7* was upregulated in the abdominal wall of animals treated with the ultrasound–microbubble-mediated gene delivery compared with that in animals without *Smad7* transfection (*Fig. 1a*). *Smad7* was localized mainly in the mesothelial and submesothelial layers of the peritoneum. Transfection mediated by ultrasound was more efficient than that without ultrasound exposure ($P<0.001$). Immunofluorescence studies using antiflag m2 antibody revealed marked staining of Smad7 protein in rats receiving *Smad7* transfection, whereas no signal was detected in no-transfection groups (*Fig. 1b*). Ultrasound significantly increased the protein synthesis of *Smad7* in the peritoneum compared with that in animals receiving no ultrasonic exposure.

Effect of Smad7 *transgene on peritoneal adhesion formation*

After death, peritoneal adhesion was graded macroscopically (*Fig. 2a*). The incidence and severity of postoperative adhesions in the various groups of experimental animals are summarized in *Table 1*. Following peritoneal abrasion, all eight rats that received adhesion alone (group 2) developed peritoneal adhesions, with grade 4 severity in seven and grade 3 severity in one animal. The percentage and severity were greatly reduced in animals that received ultrasound-mediated *Smad7* transfection ($P<0.001$ *versus* group 2). Despite the development of grade 4 adhesions in only three of the seven rats receiving *Smad7* alone (group 4), this proportion was not significantly different to that for group 2 animals ($P=0.094$). Rats receiving ultrasound alone or empty vectors showed no improvement in adhesion formation.

~~Using a novel MRI technique developed recently in the authors' laboratory[15],~~ In normal rats, the caecum moved and floated within the abdominal cavity on MRI (*Fig. 2b*). In animals with adhesions (group 2), the caecum adhered to the anterior abdominal wall with no motion, and there was no contrast medium between the adhesive caecum and the anterior abdominal wall (*Fig. 2c*); adhesion was less marked in rats treated with *Smad7* (*Fig. 2d*). The surface area of peritoneal adhesions was serially and quantitatively evaluated by MRI in (*Fig. 2e*). Peritoneal adhesions developed after the abdominal operation and progressed gradually until death. Rats treated with *Smad7* showed a

decrease in adhesion area **by 44.3, 47.7, and 43.6 per cent at 14, 21, and 28 days after operation, respectively** compared with that in animals having no treatment at the same time point (***P*=0.012, 0.007, 0.022 at day 14, 21 and 28 after operation, respectively.** MRI-determined adhesion areas before killing correlated well with evaluations at laparotomy in rats with peritoneal adhesions (r=0.97, P<0.001). Although rats grew during the observation period, no correlation was found between body weight and the surface area of peritoneal adhesions.

Effect of* Smad7 *transgene on morphological changes in the peritoneum

Histological sections of the anterior abdominal wall from normal rats demonstrated a thin submesothelial compact zone with a mesothelial monolayer ~~(*Fig. 3a,b*)~~. When adhesion occurred (group 2), the caecal smooth muscle was fused to the abdominal striated muscle with a markedly thickened submesothelial compact zone. In the *Smad7*-treated group, the abraded abdominal wall exhibited a thickened submesothelial layer with increased collagen deposition compared with peritoneum from normal control animals, but with no adhesion to the caecum. In addition, increased cellular infiltration of neutrophils and lymphocytes, as seen in group 2, was not observed in the submesothelial layer of peritoneum in animals receiving *Smad7* transfection ~~(*Fig. 3c*)~~.

Rats with surgically induced peritoneal adhesions had an increased thickness of the submesothelial compact zone of the abdominal wall compared with normal controls

(median 300 (range 150–800) *versus* 50 (40–100) μm respectively; $P<0.001$). The thickness of the submesothelial compact zone was reduced in the ultrasound-mediated *Smad7* transfection group (group 5: median 95 [range 50–300 μm]) and in the *Smad7* alone group (group 4: median 200 [range 100–650 μm)) (both $P<0.001$ *versus* adhesion but no treatment). This reduction in submesothelial thickness by *Smad7* transfection was more significant with ultrasound ($P<0.001$ *versus Smad7* transfection without ultrasound). In contrast, no significant reduction in submesothelial thickness was observed in rats receiving either ultrasound alone (median 400 [range 120–750 μm]) or empty vectors (median 300 [80–800 μm]) compared with the adhesion group receiving no treatment.

Effect of* Smad7 *transgene on extracellular matrix formation in the peritoneum

Both gene expression and protein synthesis of fibrogenic factors, including collagens I (*Fig. 3a,b*), collagen III (*Fig. 3c,d*) and fibronectin (*Fig. 3e,f*), were increased markedly in the submesothelial compact zone of the abdominal wall of rats with surgical adhesions compared with normal controls. Similarly, in peritoneal tissues the expression of α-SMA, a marker for myofibroblasts in ECM, was increased significantly in rats with adhesions (*Fig. 3g,h*). The formation of these ECM components in the peritoneum was reduced in rats treated with ultrasound-mediated *Smad7* transfection compared with that in animals receiving no treatment, ultrasound alone or empty vectors. Immunohistochemical studies confirmed increased levels of collagen I ~~(*Fig. 5a*)~~, collagen III and fibronectin ~~(data not~~

~~shown)~~, as well as α-SMA ~~(*Fig. 5b*)~~ in the submesothelial compact zone of the abraded peritoneum with or without adhesions.

Effect of* Smad7 *transgene on transforming growth factor β/Smad signalling

Compared with normal controls, both gene expression and protein synthesis of TGF-β were upregulated in the abdominal wall of rats with peritoneal adhesions (*Fig. **4***). Immunohistochemical studies confirmed increased levels of TGF-β in the submesothelial compact zone of the abdominal wall with the development of postoperative adhesions. The level of TGF-β was reduced in rats receiving ultrasound-mediated *Smad7* transfection.

The mRNA expression of Smad2 and the phosphorylated Smad2/3 protein increased significantly in the abdominal wall of rats with adhesions compared with that in normal controls (*Fig. **5**a,c*), despite no significant change in protein synthesis of Smad2 (*Fig. **5**b*). These findings indicate that the TGF-β/Smad signalling pathway was activated when the peritoneum was damaged by surgical abrasion. More importantly, phosphorylated Smad2/3 expression was decreased in rats receiving ultrasound–microbubble-mediated *Smad7* transfection, but not in those receiving *Smad7* alone, ultrasound alone or empty vectors (*Fig. **5**c*).

Discussion

This study has demonstrated that exogenous *Smad7* reduced TGF-β expression, myofibroblast activation and ECM deposition in the peritoneum. Most importantly, the *Smad7* transgene blocked Smad2/3 activation in the injured peritoneum, thereby preventing peritoneal adhesion formation.

Peritoneal adhesions develop in a large proportion of patients undergoing laparotomy (75–90 per cent) or laparoscopic surgery (13–44 per cent)[18,19]. This poses a major burden on clinical safety, health costs and medical litigation. Numerous materials, including membrane or gel barriers, dextran, hyaluronic acid and fibrinolytic agents have been examined for their ability to prevent the formation of postoperative adhesions with limited success[20]. The latest randomized controlled trial failed to demonstrate any therapeutic value for a sodium hyaluronate-based bioresorbable membrane[21]. Another randomized double-blind study showed only a 10 per cent reduction in *de novo* adhesion incidence with icodextrin (a corn starch polymer solution), which failed to prevent adhesion formation in half of the patients[22].

An understanding of the pathophysiological mechanisms of adhesion formation is essential for developing effective preventive methods. At least three mechanisms operate in adhesion formation: mesothelial injury, local inflammation, and imbalance of fibrinolytic and fibrogenic activities[23]. Their pivotal role is suggested by experimental

observations that peritoneal adhesion is attenuated by enhancing proliferation and migration of mesothelial cells[24], by suppressing T cell-induced neutrophil aggregation[14] and by neutralizing the effect of fibrogenic factors such as TGF-β[25].

In this study, the role of the TGF-β/Smad signalling pathway in the pathogenesis of peritoneal adhesion was explored. To preserve the integrity of the parietal peritoneum, peritoneal abrasion was performed rather than excision of a section of anterior abdominal wall[26]. The incidence and severity of adhesions was increased by scraping both parietal and visceral peritoneum instead of scratching either tissue alone[27]. The injured surfaces were left disjoined without sutures to enable adhesion development under natural conditions and to allow normal movement of organs or peristalsis within the peritoneal cavity, rather than apposing the injured peritoneal surfaces with mattress sutures[28].**[Author's response: This last sentence, as amended, is fine]** All animals that underwent this technique of peritoneal abrasion developed peritoneal adhesions with high-grade severity. An increase in ECM deposition, activation of myofibroblasts and Smad2/3, and TGF-β expression was observed in the injured peritoneal tissue. The study further confirmed the key role of TGF-β in stimulating myofibroblast activation and enhanced ECM formation in the development of peritoneal adhesions[29–31]. Interestingly, increased Smad2 mRNA and phosphorylated Smad2/3 protein was also observed in the injured peritoneum, demonstrating activation of the TGF-β/Smad signalling pathway.

Smad7, an inhibitory Smad, prevents the phosphorylation of Smad2 and Smad3, and then disrupts their nuclear translocalization, thereby inhibiting TGF-β signal transduction by a negative feedback loop[32]. Overexpression of *Smad7* attenuates the fibrotic effect of TGF-β and thus prevents tissue fibrosis in the kidney[11,12]. Recently, the authors successfully delivered the *Smad7* transgene into peritoneal tissues by a non-viral ultrasound–microbubble-mediated system[13]. They detected less than 10 per cent apoptotic cells and no inflammatory reaction in peritoneal tissues following this transfection, with high transfection efficiency in peritoneal tissues (approximately 80 per cent)[17]. The technique is simple and avoids the potential immunogenicity and mutagenesis that may be associated with viral gene therapy. The peak of transgene expression occurred 2 days after transfection, and transgene expression diminished in a time-dependent manner over 2 weeks. Importantly, intraperitoneal gene delivery using Tet-on inducible vector via the ultrasound–microbubble-mediated system is safe and controllable. Histological examination showed that this method did not elicit any local inflammatory reactions or cytotoxicity caused by viral vectors, as reported recently[13]. Moreover, the duration of transgene expression can be regulated by repeated administration via the peritoneal route. This promising technique of gene delivery is ideal for treating postoperative adhesions in which the dynamic and complex dysregulated repair process begins at 4–7 days and lasts for the first 2 weeks after trauma to the peritoneum[23].

Various resident cells in the peritoneum are implicated in early and late events that lead to inflammatory and fibrotic responses during the process of peritoneal insult. Proinflammatory cytokines derived from activated T cells induce a rapid but transient influx of neutrophils followed by accumulation of macrophage associated with injury of mesothelial cells[14]. Peritoneal mesothelial cells and macrophages are actively involved in peritoneal inflammation and fibrosis via TGF-β[33,34]. Overexpression of *Smad7* in T cells has been shown to prevent a murine model of glomerulonephritis by suppressing multiple effects of TGF-β[35]. As the signalling receptors TGF-βR type I and TGF-βR type II are expressed on T cells[36], TGF-β signalling in T cells is likely to be involved in T cell-mediated cell responses during the development of peritoneal adhesion. Hence, overexpression of *Smad7* may downregulate the activation of these peritoneal resident cells by inhibiting the TGF-β/Smad signalling pathway. Unlike TGF-β, which exhibits diverse effects on fibrosis and inflammation, *Smad7*, despite induction by TGF-β, has unique roles in antifibrosis by blocking TGF-β signalling (including its downstream mediator, connective tissue growth factor) and in anti-inflammation by inhibiting nuclear factor κB activation[37]. These findings signify the strategic role and therapeutic value of *Smad7* in inhibiting the TGF-β/Smad signal transduction involved in the development of postoperative peritoneal adhesions.

Interestingly, *Smad7*–microbubbles without ultrasound exposure partially inhibited

the production of fibrogenic factors and attenuated peritoneal adhesion. It is possible that microbubbles preferentially adhere to the disrupted vascular endothelium and to activated leucocytes and monocytes that are recruited along injured endothelial cells[38]. In the present model, microbubbles selectively concentrating at the damaged endothelium may collapse locally and release the preincorporated DNA. However, the efficiency of *Smad7* transfection without ultrasound was lower than that with ultrasound, signifying the role of ultrasound in enhancing the transfection efficiency. In addition, ultrasound alone exerted no inhibitory effect on adhesion formation, indicating that ultrasound *per se* has no direct therapeutic effect on adhesion formation.

By extending the previous observation that peritoneal MRI permits the delineation of peritoneal dialysis-related pathological conditions in patients undergoing peritoneal dialysis[39], the authors developed a novel MRI technique that enables an objective and serial quantitation of intra-abdominal adhesions with good correlation to laparotomy measurement[15]. In the present study, the effect of *Smad7* transfection was monitored by serial measurement of adhesion areas, and *Smad7* was found significantly to reduce adhesion formation from day 14 onwards ~~by two-fold~~. Emerging evidence has demonstrated that high spatial resolution MRI can be applied successfully in functional studies *in vivo* by depicting the recruitment of macrophages in inflamed soft-tissue infection using the magnetic contrast agent, iron oxide particles[40]. It would be interesting

further to investigate MRI of macrophages as non-invasive markers for early functional changes in peritoneal adhesion.

This novel therapeutic approach may prevent or reduce postoperative abdominal adhesions in a clinical setting. Although the treatment is at an early and experimental stage with improvements possible (such as replacing the doxycycline-driven promoter)[13,41], non-viral ultrasound–microbubble-mediated naked gene transfection may be an effective, safe and controllable technique permitting timely targeted gene delivery for the prevention of postoperative peritoneal adhesions.

Acknowledgements

H.G. was a Mrs Ivy Wu Fellow at the University of Hong Kong. The authors thank Dr M. F. Lam for surgical advice, Professor H. Y. Lan for advice on gene therapy and Ms A. W. L. Tsang for technical assistance. The study was supported by the Government Matching Grant Scheme (Hong Kong), the L & T Charitable Foundation and the House of INDOCAFE. The gene therapy delivery system has been filed under US patent publication no. US-2008-0114287-A1.

The authors declare no conflicts of interest.

References

1 Menzies D. Peritoneal adhesions. Incidence, cause, and prevention. *Surg Annu* 1992; **24**: 27–45.

2 van Goor H. Consequences and complications of peritoneal adhesions. *Colorectal Dis* 2007; **9**(Suppl 2): 25–34.

3 Menzies D, Parker M, Hoare R, Knight A. Small bowel obstruction due to postoperative adhesion: treatment patterns and associated costs in 110 hospital admissions. *Ann R Coll Surg Engl* 2001; **83**: 40–46.

4 Ellis H. Medicolegal consequences of adhesions. *Hosp Med* 2004; **65**: 348–350.

5 Harris DA, Topley N. Peritoneal adhesions. *Br J Surg* 2008; **95**: 271–272.

6 Johns A. Evidence-based prevention of post-operative adhesions. *Hum Reprod Update* 2001; 7**:** 577–579.

7 Duron JJ. Postoperative intraperitoneal adhesion pathophysiology. *Colorectal Dis* 2007; **9**(Suppl 2): 14–24.

8 di Zerega GS, Campeau JD. Peritoneal repair and post-surgical adhesion formation. *Hum Reprod Update* 2001; **7**: 547–555.

9 Savage C, Das P, Finelli AL, Townsend SR, Sun CY, Baird SE *et al*. *Caenorhabditis elegans* genes *sma-2*, *sma-3*, and *sma-4* define a conserved family of transforming growth factor beta pathway components. *Proc Natl Acad Sci U S A* 1996; **93**: 790–794.

10 Fyles AW. Dembo AJ, Bush RS, Levin W, Manchul LA, Pringle JF *et al***.** Analysis of complications in patients treated with abdomino-pelvic radiation therapy for ovarian carcinoma. *Int J Radiat Oncol Biol Phys* 1992: **22**: 847–851.

11 Li JH, Zhu HJ, Huang XR, Lai KN, Johnson RJ, Lan HY. Smad7 inhibits fibrotic effect of TGF-beta on renal tubular epithelial cells by blocking Smad2 activation. *J Am Soc Nephrol* 2002; **13**: 1464–1472.

12 Lan HY, Mu W, Tomita N, Huang XR, Li JH, Zhu HJ *et al*. Inhibition of renal fibrosis by gene transfer of inducible Smad7 using ultrasound-microbubble system in rat UUO model. *J Am Soc Nephrol* 2003; **14**: 1535–1548.

13 Guo H, Leung JC, Chan LY, Tsang AW, Lam MF, Lan HY *et al*. Ultrasound–contrast

agent mediated naked gene delivery in the peritoneal cavity of adult rat. *Gene Ther* 2007; **14**: 1712–1720.

14 Chung DR, Chitnis T, Panzo RJ, Kasper DL, Sayegh MH, Tzianabos AO. CD4+ T cells regulate surgical and postinfectious adhesion formation. *J Exp Med* 2002: **195**: 1471–1478.

15 Cheung JS, Guo H, Leung JC, Man K, Lai KN, Wu Ex. MRI visualization of rodent liver structure and peritoneal adhesion with dialyzate enhancement. *Magn Reson Med* 2008; **59**: 1170–1174.

16 Yilmaz HG, Tacyildiz IH, Keles C, Gedik E, Kilinc N. Micronized purified flavonoid fraction may prevent formation of intraperitoneal adhesions in rats. *Fertil Steril* 2005; **84**(Suppl 2): 1083–1088.

17 Guo H, Leung JC, Lam MF, Chan LY, Tsang AW, Lan HY *et al*. *Smad7* transgene attenuates peritoneal fibrosis in uremic rats treated with peritoneal dialysis. *J Am Soc Nephrol* 2007; **18**: 2689–2703.

18 Gutt CN, Oniu T, Schemmer P, Mehrabi A, Büchler MW. Fewer adhesions induced by laparoscopic surgery? *Surg Endosc* 2004; **18**: 898–906.

19 Menzies D, Ellis H. Intestinal obstruction from adhesions – how big is the problem? *Ann R Coll Surg Engl* 1990; **72**: 60–63.

20 Johns A. Evidence-based prevention of post-operative adhesions. *Hum Reprod Update* 2001; **7**: 577–579.

21 Hayashi S, Takayama T, Masuda H, Kochi M, Ishii Y, Matsuda M *et al*. Bioresorbable membrane to reduce postoperative small bowel obstruction in patients with gastric cancer: a randomized clinical trial. *Ann Surg* 2008; **247**: 766–770.

22 Brown CB, Luciano AA, Martin D, Peers E, Scrimgeour A, diZerega GS *et al*. Adept (icodextrin 4% solution) reduces adhesions after laparoscopic surgery for adhesiolysis: a double-blind, randomized, controlled study. *Fertil Steril* 2007; **88**: 1413–1426.

23 van der Wal JBC, Jeekel J. Biology of the peritoneum in normal homeostasis and after surgical trauma. *Colorectal Dis* 2007; **9**(Suppl 2): 9–13.

24 Guo Q, Li QF, Liu HJ, Li R, Wu CT, Wang LS. Sphingosine kinase 1 gene transfer reduces postoperative peritoneal adhesion in an experimental model. *Br J Surg* 2008;

95: 252–258.

25 Lucas PA, Warejcka DJ, Young HE, Lee BY. Formation of abdominal adhesions is inhibited by antibodies to transforming growth factor-beta1. *J Surg Res* 1996; **65**: 135–138.

26 Pata O, Yazici G, Apa DD, Tok E, Oz U, Kaplanoğlu M *et al.* The effect of inducible nitric oxide synthase on postoperative adhesion formation in rats. *Eur J Obstet Gynecol Reprod Biol* 2004; **117**: 64–69.

27 Wallwiener D, Meyer A, Bastert G. Adhesion formation of the parietal and visceral peritoneum: an explanation for the controversy on the use of autologous and alloplastic barriers? *Fertil Steril* 1998; **69**: 132–137.

28 Gorvy DA, Herrick SE, Shah M, Ferguson MW. Experimental manipulation of transforming growth factor-beta isoforms significantly affects adhesion formation in a murine surgical model. *Am J Pathol* 2005; **167**: 1005–1019.

29 Chegini N, Rong H, Bennett B, Stone IK. Peritoneal fluid cytokine and eicosanoid levels and their relation to the incidence of peritoneal adhesion. *J Soc Gynecol Investig* 1999; **6**: 153–157.

30 Holmdahl L, Kotseos K, Bergstrom M, Falk P, Ivarsson ML, Chegini N. Overproduction of transforming growth factor-beta1 (TGF-beta1) is associated with adhesion formation and peritoneal fibrinolytic impairment. *Surgery* 2001; **129**: 626–632.

31 Williams RS, Rossi AM, Chegini N, Schultz G. Effect of transforming growth factor beta on postoperative adhesion formation and intact peritoneum. *J Surg Res* 1992; **52**: 65–70.

32 Hayashi H, Abdollah S, Qiu Y, Cai J, Xu YY, Grinnell BW *et al*. The MAD-related protein Smad7 associates with the TGFbeta receptor and functions as an antagonist of TGFbeta signaling. *Cell* 1997; **89**: 1165–1173.

33 Noh H, Ha H, Yu MR, Kim YO, Kim JH, Lee HB. Angiotensin II mediates high glucose-induced TGF-beta1 and fibronectin upregulation in HPMC through reactive oxygen species. *Perit Dial Int* 2005; **25**: 38–47.

34 Nie J, Hao W, Dou X, Wang X, Luo N, Lan HY *et al*. Effects of *Smad7* overexpression on peritoneal inflammation in a rat peritoneal dialysis model. *Perit Dial Int* 2007; **27**: 580–588.

35 Kanamaru Y, Nakao A, Mamura M, Suzuki Y, Shirato I, Okumura K *et al*. Blockade of TGF-beta signaling in T cells prevents the development of experimental glomerulonephritis. *J Immunol* 2001; **166**: 2818–2823.

36 Schmidt-Weber CB, Letarte M, Kunzmann S, Rückert B, Bernabéu C, Blaser K. TGF-β signaling of human T cells is modulated by the ancillary TGF- β receptor endoglin. *Int Immunol* 2005, **17**: 921–930.

37 Lan HY. *Smad7* as a therapeutic agent for chronic kidney diseases. *Front Biosci* 2008; **13**: 4984–4992.

38 Villanueva FS, Jankowski RJ, Manaugh C, Wagner WR. Albumin microbubble adherence to human coronary endothelium: implications for assessment of endothelial function using myocardial contrast echocardiography. *J Am Coll Cardiol* 1997; **30**: 689–693.

39 Prischl FC, Muhr T, Seiringer EM, Funk S, Kronabethleitner G, Wallner M *et al.* Magnetic resonance imaging of the peritoneal cavity among peritoneal dialysis patients, using the dialysate as ‘contrast medium’. *J Am Soc Nephrol* 2002; **13**: 197–203.

40 Kaim AH, Jundt G, Wischer T, O'Reilly T, Frohlich J, von Schulthess GK *et al.* Functional–morphologic MR imaging with ultrasmall superparamagnetic particles of iron oxide in acute and chronic soft-tissue infection: study in rats. *Radiology* 2003; **227**: 169–174.

41 Vilaboa N, Fenna M, Munson J, Roberts SM, Voellmy R. Novel gene switches for targeted and timed expression of proteins of interest. *Mol Ther* 2005; **12**: 290–298.

Fig. 1 Expression of *Smad7* mRNA and protein in the peritoneum. **a** Quantification of *Smad7* mRNA expression in the abdominal wall by real-time reverse transcriptase–polymerase chain reaction. Values are mean(s.d.), expressed as fold change relative to normal controls. **b** Representative immunofluorescence for flag-tagged exogenous *Smad7* in the abdominal wall (original magnification ×100). Group 1, sham-operated controls; group 2, adhesion but no other treatment; group 3, adhesion plus ultrasound; group 4, adhesion plus *Smad7*; group 5, adhesion plus ultrasound and *Smad7*; group 6, adhesion plus ultrasound and empty vectors with no *Smad7*. **P*<0.050, †*P*<0.001 *versus* groups 1, 2, 3 and 5; ‡*P*<0.001 *versus* group 4 **(Tukey's multiple comparison test).**

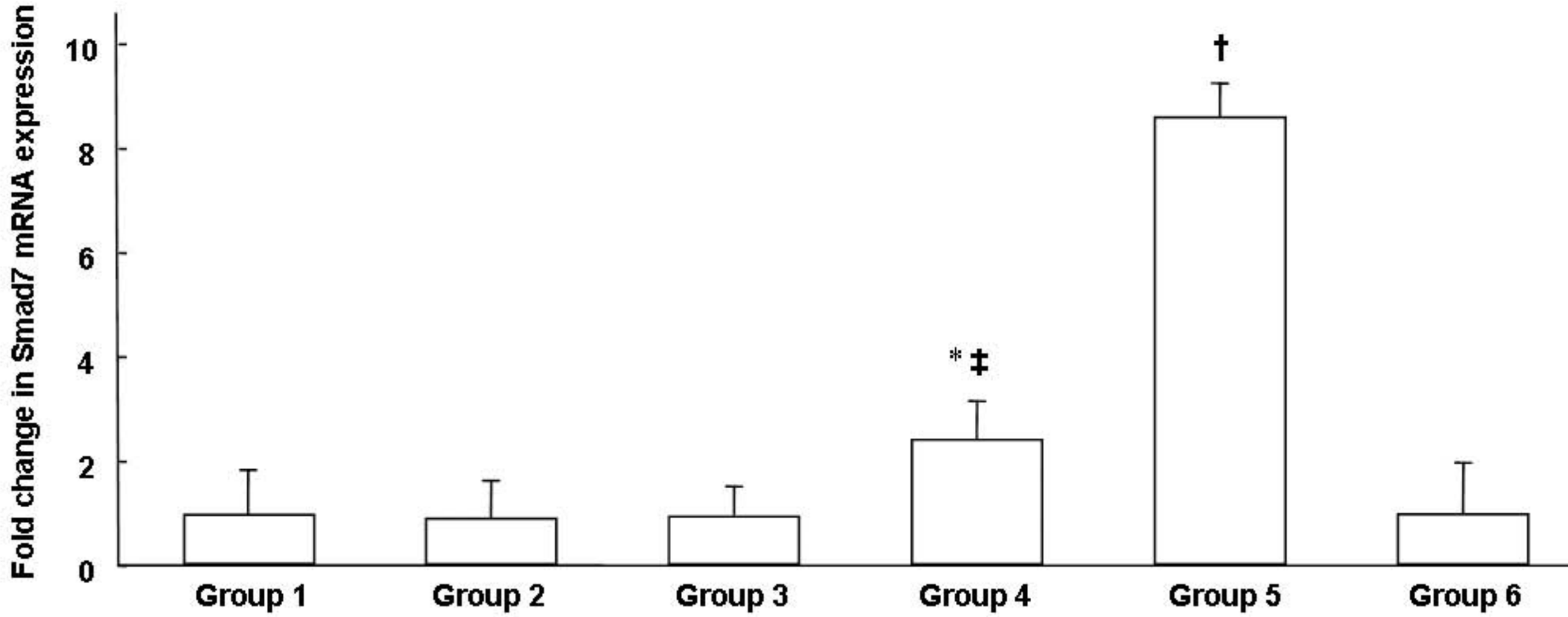

a *Smad7* mRNA expression

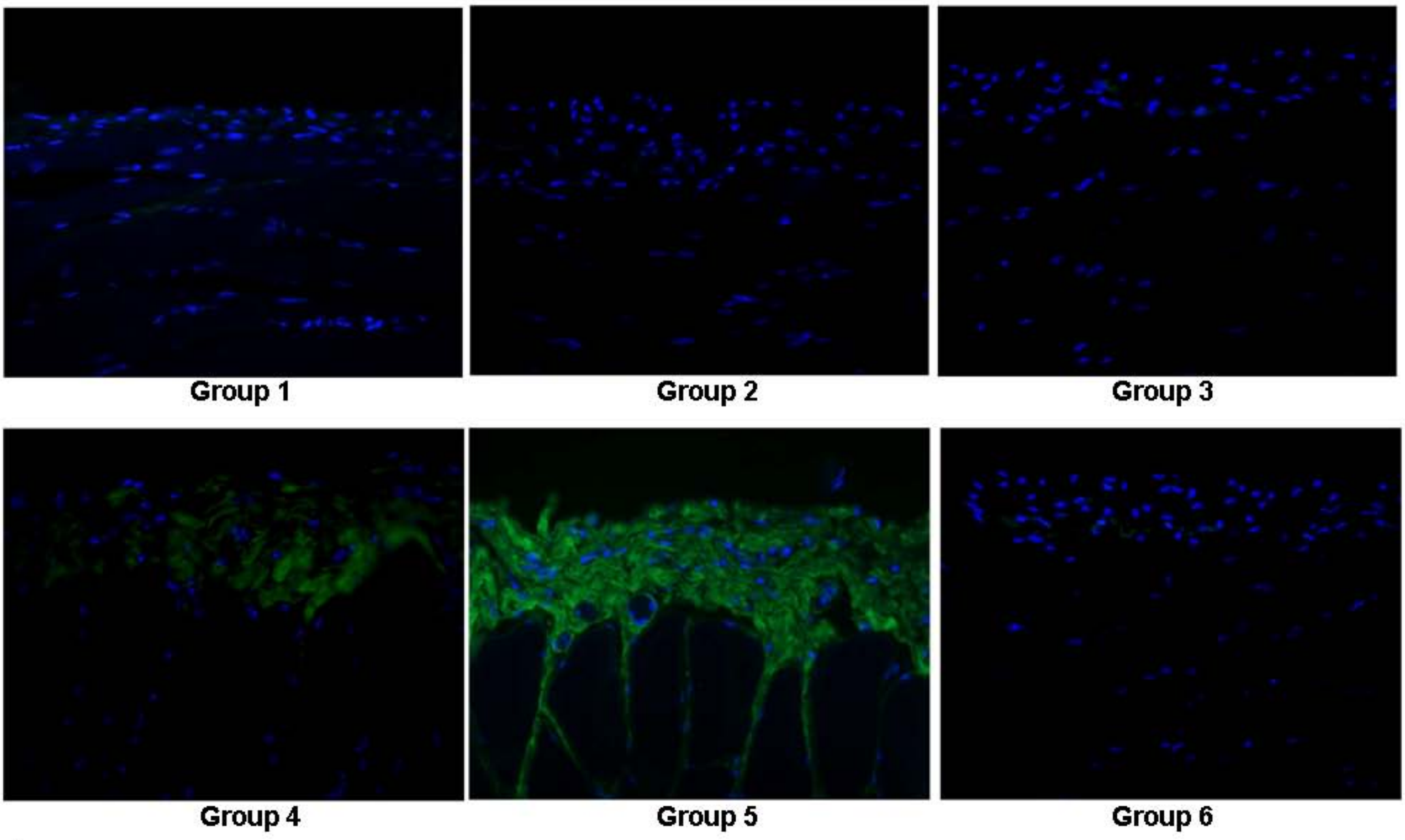

b Immunofluorescence of flag-tagged Smad7

Fig. 2 Evaluation of peritoneal adhesion by macroscopic examination and magnetic resonance imaging (MRI). **a** Grading of peritoneal adhesion by macroscopic examination. **b–d** Representative magnetic resonance images through the peritoneal cavity and corresponding macroscopic examination on day 28. Asterisks (*) indicate the caecum, and arrows denote peritoneal adhesions. **e** Serial changes in adhesion area by MRI. Values are mean(s.d.). **P*<0.050, †*P*<0.010 (adhesion plus *Smad7 versus* adhesion but no treatment, **t-test)**

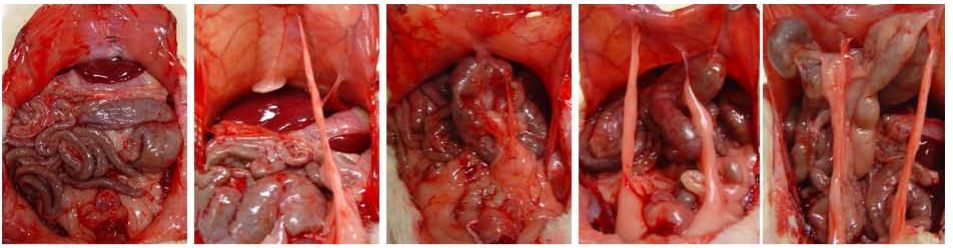

a Grade of peritoneal adhesion

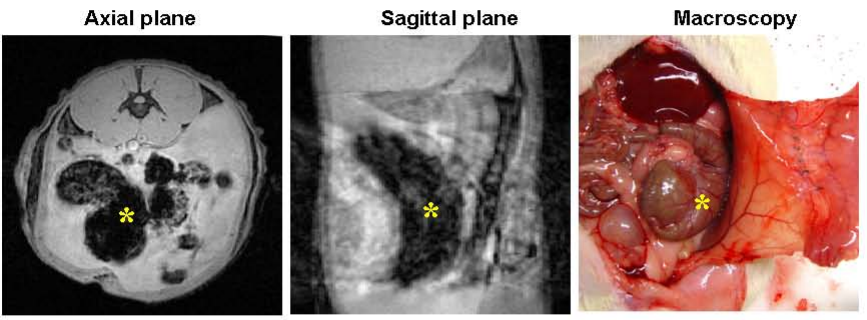

b Normal intact rat

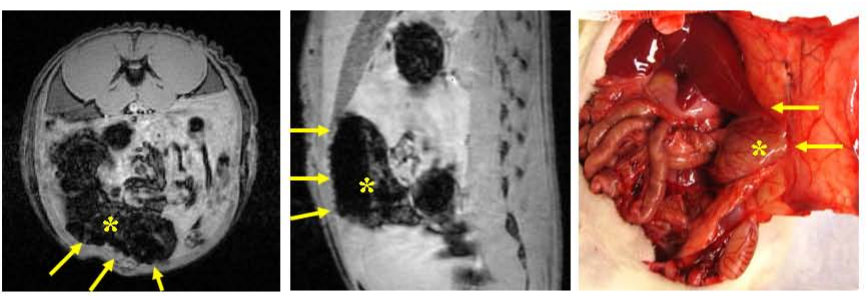

c Rat with peritoneal adhesions

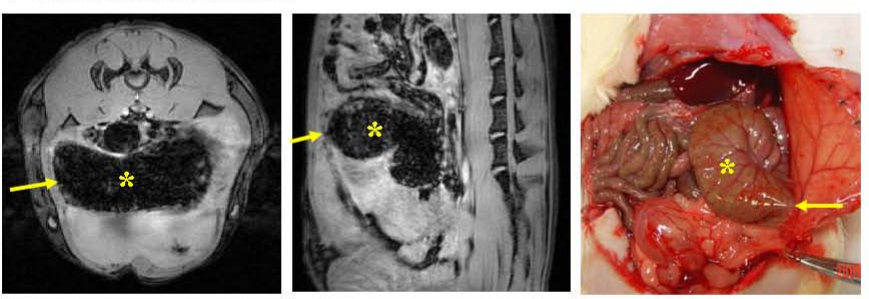

d Rat treated with *Smad7*

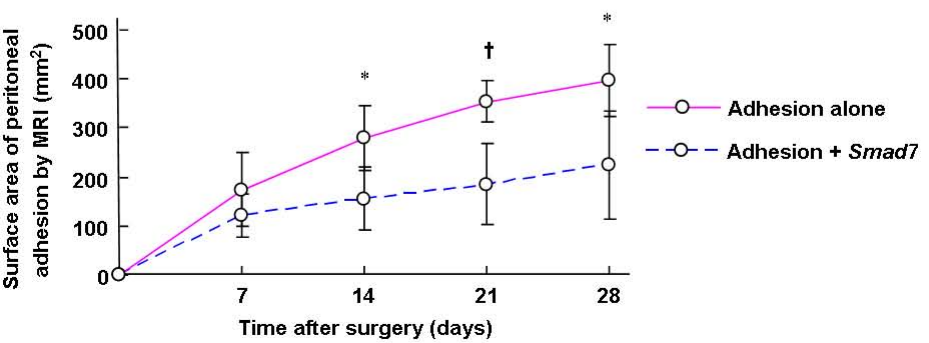

e Surface area of adhesion

~~**Fig. 3** Morphological appearance of normal peritoneum, abraded peritoneum with Smad7 treatment, and abraded peritoneum with no treatment. **a** Haematoxylin and eosin stain; **b** trichrome stain (original magnification ×50). Arrows indicate the caecal mucosa. **c** Haematoxylin and eosin stain (original magnification ×200)~~**(Author' response: agree to omit)**

Fig. 3 Gene expression and protein synthesis of extracellular matrix components in the anterior abdominal wall. Gene expression of **a** collagen I, **c** collagen III, **e** fibronectin and **g** α-smooth muscle actin (α-SMA). Protein synthesis of **b** collagen I, **d** collagen III, **f** fibronectin and **h** α-SMA. Boxes show median values with interquartile ranges, and error bars denote tenth and 90th percentiles. Group 1, sham-operated controls; group 2, adhesion but no other treatment; group 3, adhesion plus ultrasound; group 4, adhesion plus *Smad7*; group 5, adhesion plus ultrasound and *Smad7*; group 6, adhesion plus ultrasound and empty vectors with no *Smad7*. GAPDH, glyceraldehyde-3-phosphate dehydrogenase. **P*<0.050, †*P*<0.010, ‡*P*<0.001 *versus* group 1; §*P*<0.050, ¶*P*<0.010 *versus* group 2 **(Mann-Whitney U-test)**

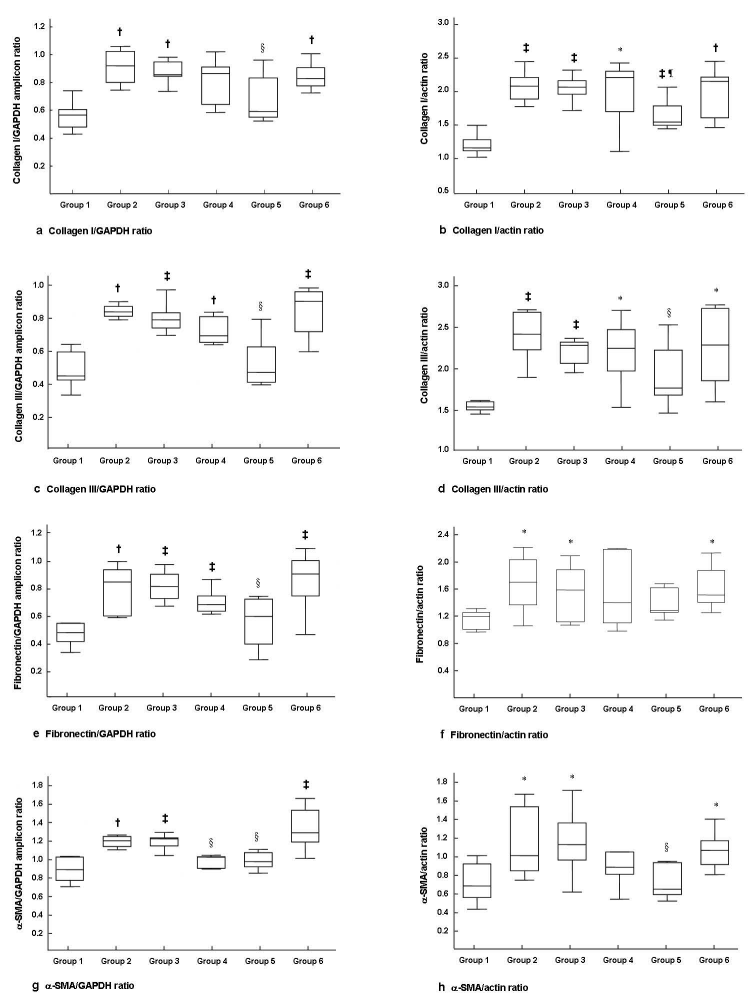

a Collagen I/GAPDH ratio

b Collagen I/actin ratio

c Collagen III/GAPDH ratio

d Collagen III/actin ratio

e Fibronectin/GAPDH ratio

f Fibronectin/actin ratio

g α-SMA/GAPDH ratio

h α-SMA/actin ratio

~~**Fig. 5** Representative immunohistochemical staining for **a** collagen I, **b** α-smooth muscle action and **c** transforming growth factor β in normal, abraded and adhesive peritoneum (original magnification ×50)~~ **(Author' response: agree to omit)**

Fig. 4 a Gene expression and **b** protein synthesis of transforming growth factor (TGF) β in the anterior abdominal wall. Boxes show median values with interquartile ranges, and error bars denote tenth and 90th percentiles. Group 1, sham-operated controls; group 2, adhesion but no other treatment; group 3, adhesion plus ultrasound; group 4, adhesion plus *Smad7*; group 5, adhesion plus ultrasound and *Smad7*; group 6, adhesion plus ultrasound and empty vectors with no *Smad7*. GAPDH, glyceraldehyde-3-phosphate dehydrogenase. **P*<0.050, †*P*<0.010, ‡*P*<0.001 *versus* group 1; §*P*<0.050 *versus* group 2 **(Mann-Whitney U-test)**

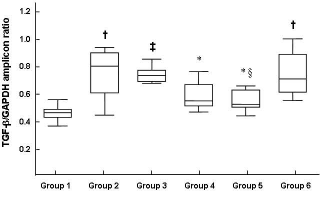

a TGF-β/GAPDH ratio

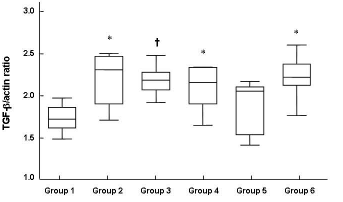

b TGF-β/actin ratio

Fig. 5 Activation of Smad2/3 in the anterior abdominal wall. **a** Gene expression of Smad2; **b** protein synthesis of Smad2; **c** protein synthesis of phosphorylated Smad2/3. Boxes show median values with interquartile ranges, and error bars denote tenth and 90th percentiles. Group 1, sham-operated controls; group 2, adhesion but no other treatment; group 3, adhesion plus ultrasound; group 4, adhesion plus *Smad7*; group 5, adhesion plus ultrasound and *Smad7*; group 6, adhesion plus ultrasound and empty vectors with no *Smad7*. GAPDH, glyceraldehyde-3-phosphate dehydrogenase. **P*<0.050, †*P*<0.010, ‡*P*<0.001 *versus* group 1; §*P*<0.010 *versus* group 2 **(Mann-Whitney U-test)**

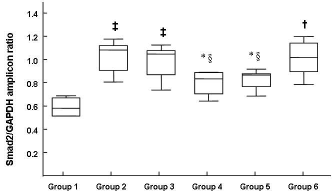

a Smad2/GAPDH ratio

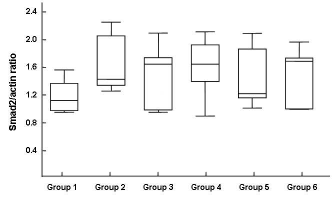

b Smad2/actin ratio

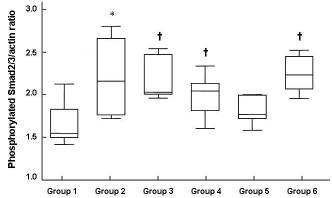

c Phosphorylated Smad2/3/actin ratio

Table 1 Adhesion formation in 48 experimental animals at 28 days

Grade	Group 1 (*n*=8)	Group 2 (*n*=8)	Group 3 (*n*=6)	Group 4 (*n*=7)	Group 5 (*n*=10)	Group 6 (*n*=9)
0	8			3	7	
1					2	
2				1		1
3		1	1		1	
4		7	5	3		8

Group 1, sham-operated controls; group 2, adhesion but no other treatment; group 3, adhesion plus ultrasound; group 4, adhesion plus *Smad7*; group 5, adhesion plus ultrasound and *Smad7*; group 6, adhesion plus ultrasound and empty vectors with no *Smad7*.